HHS Public Access

Author manuscript

J Heart Valve Dis. Author manuscript; available in PMC 2017 June 08.

Published in final edited form as:

J Heart Valve Dis. 2014 July ; 23(4): 387–394.

The Role of Inorganic Pyrophosphate in Aortic Valve Calcification

Swetha Rathan[1], **Ajit P. Yoganathan**[1,2], and **W. Charles O'Neill**[3]

[1]School of Chemical and Biomolecular Engineering, Georgia Institute of Technology, Atlanta, GA

[2]The Wallace H. Coulter Department of Biomedical Engineering, Georgia Institute of Technology, Atlanta, GA

[3]Renal Division, Emory University School of Medicine, Atlanta, GA, USA

Abstract

Background and aim of the study—Aortic valve (AV) calcification is a major cause of morbidity and mortality, yet the molecular mechanisms involved are poorly understood. Hence, an ex vivo model of calcification in intact AVs was developed in order to test the role of orthophosphate and pyrophosphate (PPi), both of which factors are known to influence vascular calcification.

Methods—Porcine AV leaflets were cultured in serum-free medium under static conditions for eight days, over which time leaflet architecture and viability were preserved. Calcification was measured as the incorporation of ^{45}Ca, with confirmation by Alizarin Red staining.

Results—Calcification required both a high phosphate concentration (3.8 mM) and removal of PPi with alkaline phosphatase or inorganic pyrophosphatase. Calcification occurred predominantly on the fibrosa and was arrested by the bisphosphonate etidronate, a non-hydrolyzable analog of PPi. Leaflets released PPi into the medium, and this was enhanced by MLS38949, a specific inhibitor of tissue non-specific alkaline phosphatase (TNAP). Furthermore, leaflets synthesized PPi from extracellular ATP, which was reduced by β, γ-methylene-ATP, an inhibitor of ectonucleotide pyrophosphorylase phosphodiesterase (NPP1).

Conclusion—The ex vivo AV calcification model developed in the present study showed that extracellular PPi, produced by valvular tissue, is a potent inhibitor of valvular calcification. In addition to synthesis, hydrolysis by TNAP also controls PPi levels and calcification. The results suggest that a decreased synthesis or increased hydrolysis of pyrophosphate may contribute to valvular calcification, and that bisphosphonates or inhibitors of TNAP are potential preventive strategies of the process. TNAP are potential preventive strategies.

Aortic valve (AV) disease is a common condition and a strong risk factor for cardiovascular deaths (1). Unfortunately, as the only currently available therapeutic option is repair or replacement of the diseased valves, there is a clear need for a preventive strategy. While the initial events in valvular disease are poorly understood and may be multifactorial,

Address for correspondence:: Ajit P. Yoganathan, The Wallace H. Coulter Department of Biomedical Engineering, Georgia Institute of Technology, 387 Technology Circle, Suite 232, Atlanta, GA 30313-2412, USA, ajit.yoganathan@bme.gatech.edu.

calcification is a common end-point that leads to valve failure (2). Thus, targeting the calcification may be a useful therapeutic strategy. Calcification likely results from an imbalance between promoters and inhibitors of mineralization; hence, an understanding of these mechanisms represents a crucial step in developing medical therapies and tissue-engineering applications.

Mineralization in other soft tissues such as arteries is controlled in large part by the concentrations of calcium and phosphate, and by endogenous inhibitors of hydroxyapatite formation. Foremost among these inhibitors is inorganic pyrophosphate (PPi), which is present in body fluids at concentrations sufficient to prevent hydroxyapatite crystal formation (3). The removal of PPi induces vascular calcification ex vivo (4), and PPi can prevent vascular calcification both ex vivo and in vivo (5). Recently, PPi was also found to inhibit the calcification of interstitial cells cultured from AVs (6).

PPi is produced extracellularly from ATP through the action of ectonucleotide pyrophosphatase/pyrophosphorylase (NPP1) (7), and absence of this enzyme results in severe fatal arterial calcification (8). PPi may also be transported out of cells via the membrane protein ANK, an absence of which also causes ectopic calcification (9). A key determinant of extracellular PPi levels and mineralization is tissue non-specific alkaline phosphatase (TNAP), an ecto-enzyme that hydrolyzes PPi. It is the robust expression of TNAP by osteoblasts that lowers local PPi levels and enables bone formation to occur (10). However, an increased activity of TNAP in vascular smooth muscle may contribute to the vascular calcification that occurs in renal failure (11).

Thus, it was hypothesized that PPi has a similarly important role in preventing AV calcification. While pyrophosphate was found to inhibit calcification in interstitial cells cultured from AV leaflets (6), cell culture does not reflect events and metabolism in intact tissues. Consequently, an ex vivo calcification model was developed which used cultured porcine AV leaflets, and this was employed to examine PPi metabolism and its effect on calcification.

Materials and methods

Tissue harvest and preparation

Hearts were obtained from healthy, non-pregnant female pigs immediately after slaughter at a local abattoir (Holifield Farms, Covington, GA, USA). The AV leaflets were immediately excised, thoroughly rinsed, and stored in sterile Dulbecco's phosphate-buffered solution (dPBS; Sigma, St. Louis, MO, USA) at 4°C for transport to the laboratory. Upon arrival at the laboratory, five pieces (each 5 mm^2) were cut aseptically from the basal region of each leaflet in a laminar flow hood. Each leaflet sample was placed in a separate well of a 12-well tissue culture plate with 2.4 ml of Dulbecco's modified Eagle medium (DMEM; Mediatech, Herndon, VA, USA) containing penicillin and streptomycin for eight days in a 5% CO_2 incubator at 37°C, with media changes every two days. The DMEM contains 1.8 mM calcium and 0.8 mM phosphate, and the phosphate concentration was increased by adding NaH_2PO_4. For some studies, the valves were devitalized prior to culture by repetitive freezing and thawing (five to six cycles). The following additives were used when indicated:

inorganic pyrophosphatase (from bakers' yeast; Sigma Diagnostics, St. Louis, MO, USA), 1000 Units/ml stock solution in Hanks buffered salt solution; calf intestinal alkaline phosphatase (Promega, Madison, WI, USA), 1000 units/ml suspension; and etidronic acid (TCI America, Portland, OR, USA), 1 mM stock solution in distilled water.

Calcium incorporation

This was monitored as described previously (4). Approximately 0.3 μCi/ml of $^{45}CaCl_2$ (DuPont-NEN, Boston, MA, USA) was added to the culture medium; on completion of culture, the tissues were washed briefly twice and then incubated for 60 min in a physiologic salt solution at room temperature to remove any soluble tissue calcium. The samples were dried in an oven, weighed, and then extracted overnight in 500 μl of 1 M HCl to remove any incorporated ^{45}Ca for subsequent measurement by liquid scintillation counting. The results were expressed as nanomoles of calcium per mg tissue, calculated from the specific activity of ^{45}Ca in the medium.

Histological assessment

The tissues were rinsed briefly in Hanks buffered salt solution and then fixed in 10% neutral buffered formalin (Fisher Scientific, Suwanee, GA, USA) for at least 24 h, saturated in 70% ethanol, processed in ascending grades of ethanol, embedded in paraffin, and cut into sections, each of 5 μm thickness. The tissue slices were stained with hematoxylin and eosin (H&E) stains, using standard protocols. Alizarin Red staining was performed with a 2% solution in distilled water at pH 4.1–4.3 for up to 5 min. The Verhoeff-Van Gieson elastin stain was performed using a kit (Sigma-Aldrich, St. Louis, MO, USA) according to the manufacturer's directions.

Viability staining was performed by incubating tissues with 0.5 mg/ml methylthiazoletetrazolium (MTT; Sigma Aldrich) in DMEM at the end of the culture period for 3 h at 37°C, followed by three washes in PBS and embedding for frozen sectioning.

Cell apoptosis staining was performed using the In Situ Cell Death Detection Kit; TMR red, TUNEL kit (Roche Diagnostics, Mannheim, Germany). Cryopreserved tissue sections were fixed with 4% paraformaldehyde in dPBS (pH 7.4) for 20 min, rinsed with dPBS for 30 min, permeabilized with 0.1% Triton X-100 (Sigma-Aldrich) in dPBS (2 min at 4°C), and rinsed twice with dPBS. Staining was performed by incubating the tissue sections for 1 h at 37°C in a humidified chamber in the dark in 50 μl of TUNEL reaction mixture, followed by counterstaining with DAPI for 5 min. A positive control was prepared by incubating the fixed and permeabilized tissue section with DNAse-I solution [3–3000U/ml RNAse-free DNAse-I (Qiagen, Valencia, CA, USA) in 50 mM Tris-Cl (Sigma-Aldrich), pH 7.5, 1 mg/ml bovine serum albumin (BSA; Fisher Scientific, Pittsburgh, PA, USA)] for 10 min prior to labeling with the TUNEL reaction mixture. A negative control was prepared by incubating fixed and permeabilized tissue sections in 50 μl of TUNEL label solution (without terminal transferase).

A Nikon E600 imaging microscope (Nikon Inc., Melville, NY, USA) coupled to a Retiga 1300C camera (I-Cube, Glen Burnie, MD, USA) and its bundled software (Q-Capture Pro) were used to acquire images.

Pyrophosphate production

Fresh AV leaflets were incubated in DMEM (three leaflets in 1 ml) in a 5% CO_2 incubator at 37°C with or without 30 μM MLS38949, a specific inhibitor of TNAP (12) (PubChem ID 2931238, kindly provided by Dr. Jose Luis Millan, Sanford-Burnham Biomedical Research Institute, La Jolla, CA, USA). The PPi content of the medium was measured enzymatically using uridine-diphospho (UDP) glucose pyrophosphorylase and UDP[^{14}C]glucose as substrate, as described previously (13). The synthesis of PPi from ATP was measured by incubating fresh leaflets in physiologic salt solution (two leaflets in 1 ml) containing 3 nM ATP and tracer [γ^{32}P] ATP with or without 300 μM β, γ-methylene ATP (an inhibitor of NPP1) or 30 μM MLS38949. Samples of the medium were spotted onto polyethyleneimine-cellulose plates (Sigma-Aldrich), followed by development with 650 mM KH_2PO_4 (pH 3). Spots identified by autoradiography were scraped into distilled water and counted as Cerenkov radiation by liquid scintillation. PPi production was normalized to the dry weight of the leaflets.

Statistical analysis

Data were expressed as mean ± SE of at least six samples. The normality of all the data was tested using the Anderson-Darling method. Student's *t*-test was used for comparison of two groups, and a one-way ANOVA with Tukey's post-hoc test was used for comparisons between multiple groups. If not normally distributed, the data were analyzed using Mann-Whitney or Kruskal-Wallis tests. Differences between samples were considered significant when the p-value was <0.05.

Results

Effect of phosphate and phosphatases on AV calcification ex vivo

The incorporation of ^{45}Ca into AV leaflets cultured with different phosphate concentrations for eight days is shown in Figure 1A. A small uptake of ^{45}Ca occurred without added phosphate that probably represents equilibration with cellular stores, as described previously for cultured aortas (4). The incorporation of ^{45}Ca was increased at 3.2 mM phosphate and became significant at 3.8 mM ($p < 0.05$ versus 0.8 mM), but no staining was apparent with Alizarin Red. Incorporation of ^{45}Ca was markedly increased by the addition of 0.4 units/ml of inorganic pyrophosphatase (IP) to the medium, and this resulted in a positive Alizarin Red staining (Fig. 1B), indicating that this represented calcification. A prior dose-response study showed that this concentration of IP would result in maximal calcification (not shown). The increased ^{45}Ca incorporation was apparent by two days (Fig. 1C), and was visible by Alizarin Red staining after four days (Fig. 1D). Staining occurred predominantly on the fibrosa side of the leaflet with occasional minor staining of the ventricularis.

Similar results were obtained when alkaline phosphatase (ALP) was added to the cultures (see Fig. 2). ALP hydrolyzes PPi but is less specific and also hydrolyzes other phosphorylated compounds (14). ALP + IP did not produce any further calcification beyond IP alone, indicating that this effect was solely through the removal of PPi. Lastly, devitalization of the leaflets also induced significant calcification ($p = 0.05$ versus control).

Effect of etidronate on AV calcification ex vivo

In order to confirm that the effect of IP was indeed due to the removal of PPi, the bisphosphonate etidronate (a non-hydrolyzable analog of PPi) (15) was added to the culture medium. Etidronate completely prevented AV leaflet calcification at a concentration as low as 0.07 μM (Fig. 3).

AV structure and cell viability ex vivo

There were no apparent histologic changes in the leaflets after culture for eight days, as revealed by staining with H&E (not shown) or Verhoeff-Van Gieson staining for elastin (Fig. 4A). Staining with MTT (Fig. 4B) indicated that cell viability of AV tissues was maintained during culture. As expected, there was no staining in devitalized leaflets. Consistent with MTT results, TUNEL staining did not reveal any apoptotic cells (Fig. 4C). The addition of phosphate, IP, ALP or etidronate had no effect on either the histology or viability of the cells.

Synthesis of pyrophosphate by AV leaflets

The AV leaflets were capable of producing PPi, as shown by the appearance of PPi (measured by enzyme assay) in the medium (Fig. 5A). MLS38949, an inhibitor of tissue non-specific alkaline phosphatase (TNAP), was added to prevent hydrolysis of PPi. There was a rapid appearance of PPi within the first hour and, in the presence of MLS38949, this continued to increase.

NPP1 is the principal synthetic enzyme for extracellular PPi, and to determine whether it is active in valve tissue, freshly isolated leaflets were incubated with [γ^{32}P]ATP. The disappearance of ATP was rapid and complete by 5 min, with most ATP hydrolyzed to orthophosphate (Fig. 5B and C). However, a small amount of ^{32}PPi was apparent, and this was reduced on the addition of β, γ-methylene ATP, an inhibitor of NPP1 (16), indicating that ^{32}PPi was being synthesized by the leaflets and was not merely a contaminant of the [γ^{32}P]ATP. The amount of ^{32}PPi was significantly increased when the TNAP inhibitor MLS38949 was added.

Discussion

Valve leaflets cultured under serum-free conditions maintained viability and normal morphology for at least eight days. Under these conditions, calcification required an elevated phosphate concentration and the addition of inorganic pyrophosphatase. This calcification occurred mostly in the fibrosa, as seen in humans in vivo, although there was occasional calcification of the ventricularis portion. This is consistent with previous clinical and experimental findings that the fibrosa is more prone to mineralization compared to the ventricularis (17). In AVs from patients with end-stage renal disease, which is a hyperphosphatemic, low-pyrophosphate condition (18), calcification occurred also primarily within the fibrosa with an occasional involvement of the ventricularis (W. C. O'Neill, unpublished data).

The effect of phosphate is likely due to the promotion of Ca_2HPO_4 crystallization and subsequent hydroxyapatite formation (3), but phosphate may also induce cellular changes including osteogenic differentiation that may promote mineralization (19). Serum phosphate is a known risk factor for valvular calcification in chronic kidney disease (20,21). The requirement of IP is probably related to the removal of PPi, a critical endogenous inhibitor of calcification. The inhibition of calcification by etidronate, a non-hydrolyzable PPi analog, is consistent with this. Unlike IP, which selectively hydrolyzes PPi, ALP can hydrolyze other phosphorylated compounds as well such as osteopontin, another endogenous inhibitor of calcification (14). The fact that ALP did not produce additional calcification when added with IP suggests that other phosphorylated inhibitors are not active in cultured AV leaflets. The significant calcification after devitalization is consistent with loss of calcification inhibitors, although cell necrosis could become a nidus for dystrophic calcification (22).

This role of PPi in inhibiting AV calcification is consistent with the results of a previous study in cultured valvular interstitial cells (6), and with the known inhibitory role of PPi in vascular calcification. Similar effects of IP and ALP were observed in cultured aortas (4,11), and bisphosphonates - which are non-hydrolyzable analogs of PPi - also prevent vascular calcification in culture and in vivo (23,24).

Although PPi is present in the circulation at concentrations that can inhibit calcification (3), it is clear from the results obtained that valve tissue can synthesize PPi that could act locally. Valve leaflets generated PPi from added ATP, which was significantly decreased in the presence of β, γ-methylene ATP, an inhibitor of NPP1. The latter is a major source of extracellular PPi, and a deficiency of NPP1 results in severe arterial calcification in humans (25) and mice (8). Since β, γ-methylene ATP interferes with the assay of PPi, it is not possible to determine the contribution of NPP1 to net PPi synthesis by the leaflets. Another potential source of extracellular PPi is the putative membrane transporter ANK although, as there are no known inhibitors, its contribution also cannot be determined.

Paradoxically, NPP1 expression is increased in calcified valves (7) and has been proposed to promote calcification by reducing extracellular ATP levels (thereby promoting apoptosis) and increasing phosphate levels. However, the studies supporting this were performed in cultured cells and the amount of phosphate that could be generated from extracellular ATP is minimal compared to ambient phosphate levels. While this remains a possible mechanism, the current results demonstrate that a simple removal of PPi without altering NPP1 is sufficient to produce calcification, indicating that NPP1 activity is required to prevent calcification. It is possible that the increased NPP1 expression in calcified valves is a compensatory response to the calcification or a local deficiency of PPi.

TNAP hydrolyzes PPi and also regulates the availability of PPi in the vascular tissues (10), being responsible for almost 50% of the PPi hydrolysis in vascular smooth muscle. The inhibition of TNAP significantly increased the production of PPi by AV leaflets, indicating that this enzyme also influences the levels of PPi in the AV. Consistent with this, elevated ALP activity has also been reported in calcified valves (26).

Study limitations

This tissue-based model offers substantial advantages over cultured cells because a normal extracellular matrix and both valve interstitial and endothelial cells are present. In addition, the serum-free culture medium avoids potential problems related to the myriad of growth factors, cytokines and compounds present in serum. The absence of serum did not affect cell viability. One limitation, however, was that the cultures were performed under static conditions, which does not reflect the dynamic mechanical environment in vivo that differs on either side of the leaflets. Yet, even in static cultures, the results showed that AV leaflets are capable of producing PPi, the levels of which are intricately regulated by the expression of ENPP1 and TNAP. As mechanical stimuli have significant effects on cell metabolism in valve tissue (27), the metabolism of PPi is likely also to be affected, and this will require further study.

In conclusion, the results of the present study demonstrated a critical role for pyrophosphate in AV calcification, and also suggested important roles for NPP1 and TNAP in controlling PPi levels in valvular tissues. Thus, agents that enhance NPP1 activity or inhibit TNAP could be potential therapies. Although PPi could be administered to treat AV calcification, it is subject to rapid hydrolysis in vivo (5). Bisphosphonates, which are non-hydrolyzable analogs of pyrophosphate and have been shown to inhibit vascular calcification in animal models, are a potential alternative but could have unknown effects on bone metabolism.

Acknowledgments

The authors thank Holifield Farms (Covington, GA, USA) for supplying porcine hearts, Georgia Tech undergraduate researchers Shan Lee and Anita Rajamani for their help with the histology, and Aqua Asberry (Georgia Tech Histology Laboratory Coordinator) for her expert guidance with elastin stains.

This research was supported by the American Heart Association under the Predoctoral Research Award 12PRE11750044 (Swetha Rathan), American Heart Association Grant-In-Aid #11GRNT7660009 (W. C. O'Neill), Discretionary Chair Funds of Ajit P. Yoganathan, and generous donations to the Yoganathan laboratory by Tom Shirley and Gurley.

Dr. O'Neill is a co-inventor of a patent owned by Emory University related to the therapeutic use of pyrophosphate.

References

1. Lindroos M, Kupari M, Heikkila J, Tilvis R. Prevalence of aortic valve abnormalities in the elderly: An echocardiographic study of a random population sample. J Am Coll Cardiol. 1993; 21:1220–1225. [PubMed: 8459080]
2. O'Brien KD. Pathogenesis of calcific aortic valve disease: A disease process comes of age (and a good deal more). Arterioscler Thromb Vasc Biol. 2006; 26:1721–1728. [PubMed: 16709942]
3. Meyer JL. Can biological calcification occur in the presence of pyrophosphate? Arch Biochem Biophys. 1984; 231:1–8. [PubMed: 6326671]
4. Lomashvili KA, Cobbs S, Hennigar RA, Hardcastle KI, O'Neill WC. Phosphate-induced vascular calcification: Role of pyrophosphate and osteopontin. J Am Soc Nephrol. 2004; 15:1392–1401. [PubMed: 15153550]
5. O'Neill WC, Lomashvili KA, Malluche HH, Faugere M-C, Riser BL. Treatment with pyrophosphate inhibits uremic vascular calcification. Kidney Int. 2011; 79:512–517. [PubMed: 21124302]
6. Côté N, El Husseini D, Pépin A, et al. ATP acts as a survival signal and prevents the mineralization of aortic valve. J Mol Cell Cardiol. 2012; 52:1191–1202. [PubMed: 22366713]

7. Harmey D, Hessle L, Narisawa S, Johnson KA, Terkeltaub R, Millán JL. Concerted regulation of inorganic pyrophosphate and osteopontin by Akp2, Enpp1, and Ank: An integrated model of the pathogenesis of mineralization disorders. Am J Pathol. 2004; 164:1199–1209. [PubMed: 15039209]
8. Johnson K, Polewski M, van Etten D, Terkeltaub R. Chondrogenesis mediated by PPi depletion promotes spontaneous aortic calcification in NPP1 −/− mice. Arterioscler Thromb Vasc Biol. 2005; 25:686–691. [PubMed: 15625282]
9. Ho AM, Johnson MD, Kingsley DM. Role of the mouse ank gene in control of tissue calcification and arthritis. Science. 2000; 289:265–270. [PubMed: 10894769]
10. Murshed M, Harmey D, Millán JL, McKee MD, Karsenty G. Unique coexpression in osteoblasts of broadly expressed genes accounts for the spatial restriction of ECM mineralization to bone. Genes Dev. 2005; 19:1093–1104. [PubMed: 15833911]
11. Lomashvili KA, Garg P, Narisawa S, Millan JL, O'Neill WC. Upregulation of alkaline phosphatase and pyrophosphate hydrolysis: Potential mechanism for uremic vascular calcification. Kidney Int. 2008; 73:1024–1030. [PubMed: 18288101]
12. Dahl R, Sergienko EA, Su Y, et al. Discovery and validation of a series of aryl sulfonamides as selective inhibitors of tissue-nonspecific alkaline phosphatase (TNAP). J Med Chem. 2009; 52:6919–6925. [PubMed: 19821572]
13. O'Neill WC, Sigrist MK, McIntyre CW. Plasma pyrophosphate and vascular calcification in chronic kidney disease. Nephrol Dial Transplant. 2010; 25:187–1891. [PubMed: 19633093]
14. Golub EE, Boesze-Battaglia K. The role of alkaline phosphatase in mineralization. Curr Opin Orthopaed. 2007; 18:444–448.
15. Fleisch H. Bisphosphonates: Mechanisms of action. Endocr Rev. 1998; 19:80–100. [PubMed: 9494781]
16. Joseph SM, Pifer MA, Przybylski RJ, Dubyak GR. Methylene ATP analogs as modulators of extracellular ATP metabolism and accumulation. Br J Pharmacol. 2004; 142:1002–1014. [PubMed: 15210578]
17. Freeman RV, Otto CM. Spectrum of calcific aortic valve disease: Pathogenesis, disease progression, and treatment strategies. Circulation. 2005; 111:3316–3326. [PubMed: 15967862]
18. Lomashvili KA, Khawandi W, O'Neill WC. Reduced plasma pyrophosphate levels in hemodialysis patients. J Am Soc Nephrol. 2005; 16:2495–2500. [PubMed: 15958726]
19. Peng A, Wu T, Zeng C, et al. Adverse effects of simulated hyper- and hypo-phosphatemia on endothelial cell function and viability. PLoS ONE. 2011; 6:e23268. [PubMed: 21858050]
20. Petrović D, Obrenović R, Stojimirović B. Risk factors for aortic valve calcification in patients on regular hemodialysis. Int J Artif Organs. 2009; 32:173–179. [PubMed: 19440993]
21. Hruska KA, Mathew S, Lund R, Qiu P, Pratt R. Hyperphosphatemia of chronic kidney disease. Kidney Int. 2008; 74:148–157. [PubMed: 18449174]
22. Amann K. Media Calcification and intima calcification are distinct entities in chronic kidney disease. Clin J Am Soc Nephrol. 2008; 3:1599–1605. [PubMed: 18815240]
23. Fleisch HA, Russell RGG, Bisaz S, Mühlbauer RC, Williams DA. The inhibitory effect of phosphonates on the formation of calcium phosphate crystals in vitro and on aortic and kidney calcification in vivo. Eur J Clin Invest. 1970; 1:12–18. [PubMed: 4319371]
24. Koba AL, Marie-Claude M-F, Xiaonan W, Hartmut HM, O'Neill WC. Effect of bisphosphonates on vascular calcification and bone metabolism in experimental renal failure. Kidney Int. 2009; 75:617–625. [PubMed: 19129793]
25. Rutsch F, Vaingankar S, Johnson K, et al. PC-1 Nucleoside triphosphate pyrophosphohydrolase deficiency in idiopathic infantile arterial calcification. Am J Pathol. 2001; 158:543–554. [PubMed: 11159191]
26. Clark-Greuel JN, Connolly JM, Sorichillo E, et al. Transforming growth factor-β1 mechanisms in aortic valve calcification: increased alkaline phosphatase and related events. Ann Thorac Surg. 2007; 83:946–953. [PubMed: 17307438]
27. Arjunon S, Rathan S, Jo H, Yoganathan A. Aortic valve: Mechanical environment and mechanobiology. Ann Biomed Eng. 2013:1–16.

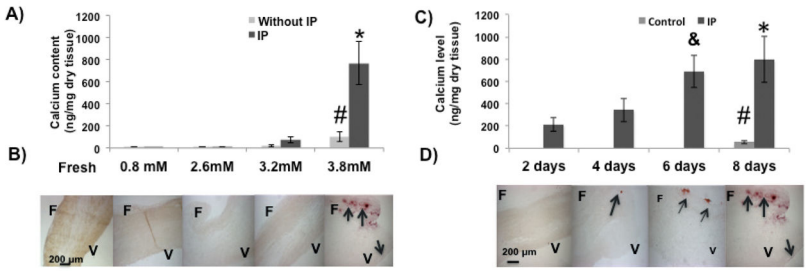

Figure 1.

Effect of phosphate and pyrophosphatase on calcification of aortic valve leaflets ex vivo. A). Incorporation of ^{45}Ca in valve tissues over eight days at different phosphate concentrations with or without inorganic pyrophosphatase (IP). # $p < 0.05$ versus 0.8 mM phosphate alone; * $p < 0.05$ versus 3.8 mM phosphate alone (n = 8). B) Corresponding alizarin red stains for valves cultured with IP. A freshly isolated leaflet is included as a negative control (far left). F: Fibrosa; V: Ventricularis. The arrows point to calcified areas. C) Time course of ^{45}Ca incorporation in valve tissues cultured with or without IP and 3.8mM PO_4^{3-}; * $p < 0.05$ versus 2, 4 days; & $p < 0.1$ versus 4 days; # $p < 0.05$ versus 4, 6, 8 days (n = 8). D) Corresponding alizarin red stains.

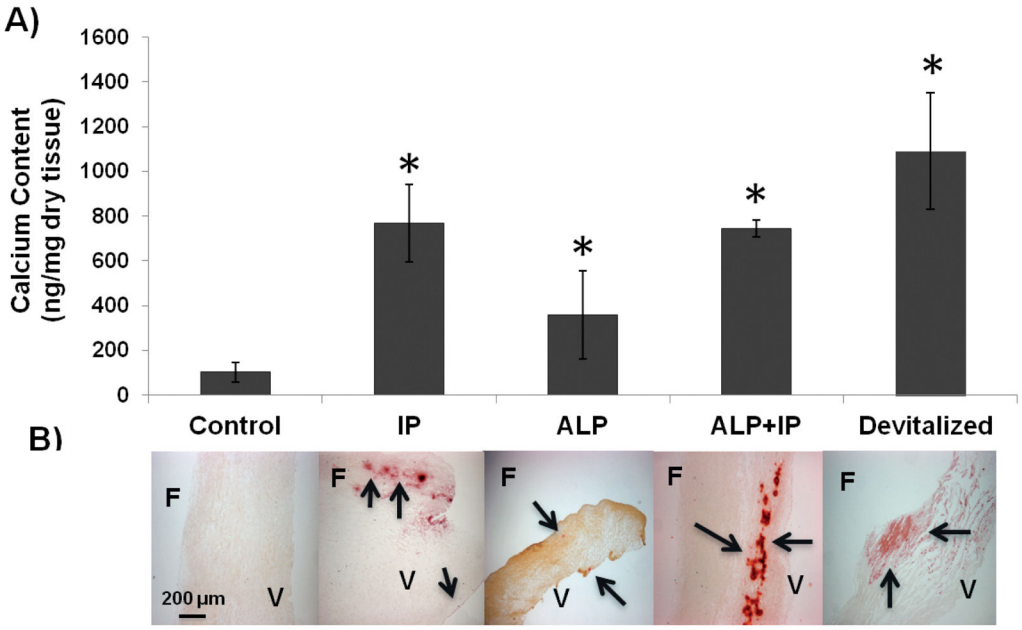

Figure 2.

Effect of phosphatases and devitalization on calcification of AV leaflets ex vivo. A) Incorporation of ^{45}Ca into AV leaflets cultured in different conditions as indicated. Control refers to leaflets cultured with 3.8 mM PO_4^{3-} only. IP: Inorganic pyrophosphatase; ALP: Alkaline phosphatase; Leaflets were devitalized by freezing and thawing several times. * $p < 0.05$ versus control ($n = 8$). B) Corresponding alizarin red stains. F: Fibrosa; V: Ventricularis. The arrows point to calcified areas.

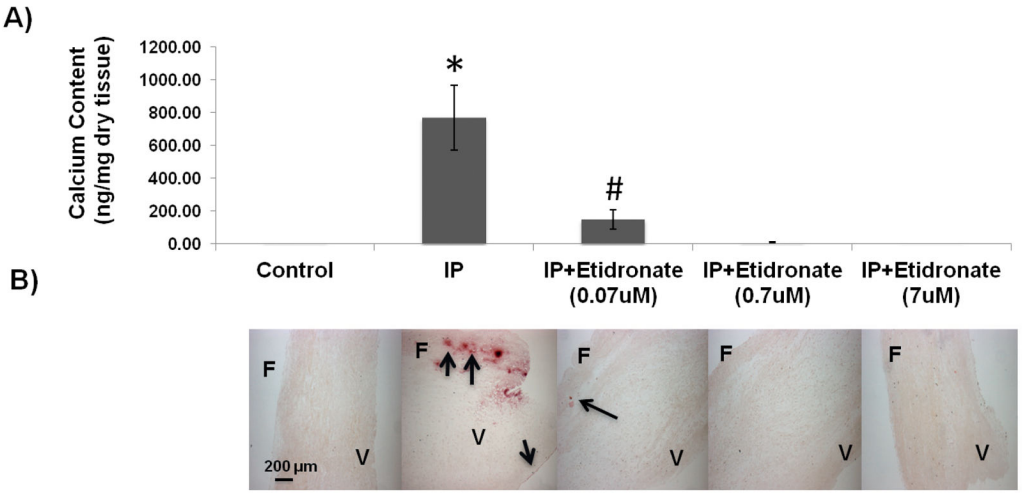

Figure 3.

Effect of etidronate on calcification of AV leaflets ex vivo. A) Incorporation of ^{45}Ca into valve leaflets over eight days at different concentrations of etidronate with inorganic pyrophosphatase (IP) and 3.8 mM PO_4^{3-}; * $p < 0.05$ versus all other groups; # $p < 0.05$ versus 3.8 mM phosphates only and other concentrations of etidronate. B) Corresponding alizarin red stains. The arrows point to calcified areas. F: Fibrosa; V: Ventricularis.

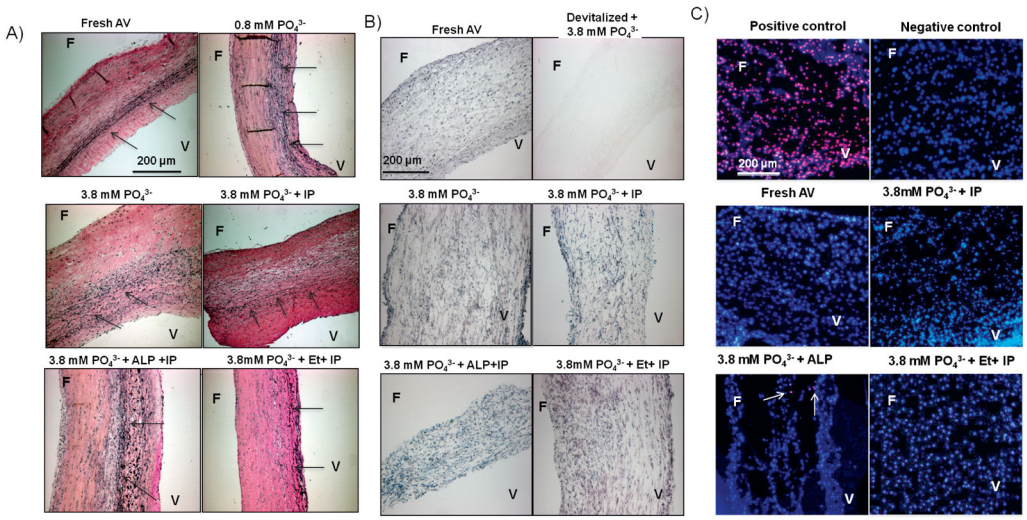

Figure 4.

AV structure and cell viability ex vivo. A) Verhoeff-Van Gieson elastin stain shows preserved AV structure under all culture conditions. The arrows point to elastin fibers oriented along the length of the tissue. B) MTT stain shows preserved viability of AV tissue under all culture conditions. Leaflets were devitalized by freezing and thawing several times; a negative control showed no staining. C) TUNEL stain for apoptosis. Apoptotic nuclei stain red superimposed on the blue DAPI counterstain. Positive control: After treatment with DNAse; Negative control: Without TMR red stain. The arrows point to apoptotic cells. Fresh and cultured leaflets each had less than 0.2% positive cells (of >500 counted). F: Fibrosa; V: Ventricularis; IP: Inorganic pyrophosphatase; ALP: Alkaline phosphatase; Et: Etidronate.

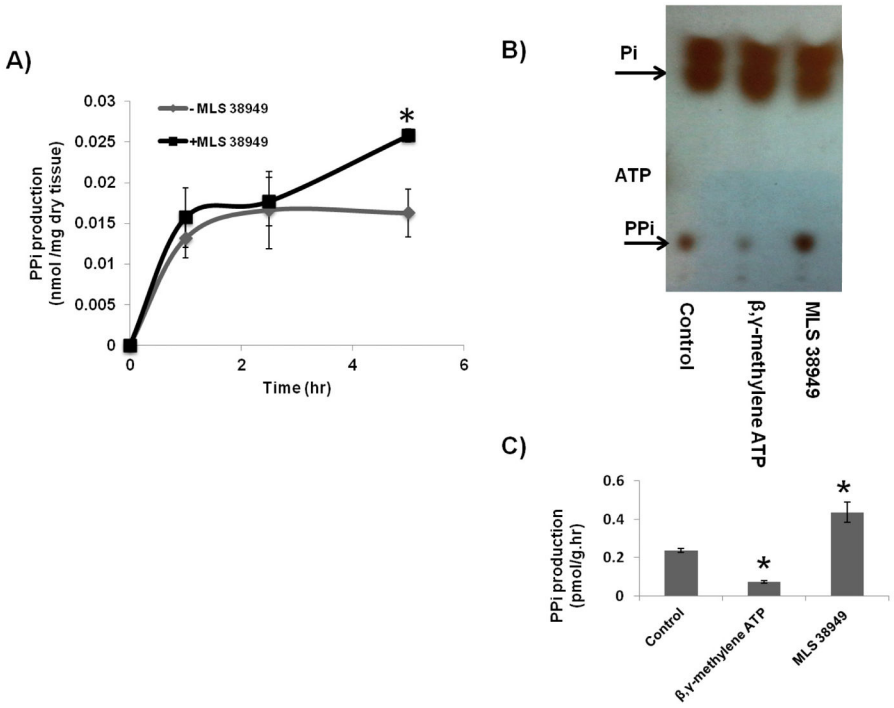

Figure 5.

Synthesis of pyrophosphate from AV leaflets. A) Quantification of PPi released into the medium from AV leaflets incubated with or without 30 μM MLS38949 (an inhibitor of TNAP) as a function of time. * $p < 0.05$ versus no MLS38949 at 5 h ($n = 4$). B) Autoradiogram of a representative thin-layer chromatogram after incubation of valve leaflets with [γ^{32}P]ATP in 3 nM ATP with or without 30 μM MLS38949 or 300 μM β, γ-methylene ATP, an inhibitor of NPP1. All of the exogenous ATP was consumed in 5 min. Control leaflets were incubated without any inhibitors. C) Quantification of PPi production by AV tissue from ATP. * $p < 0.05$ versus control.